Energy and Electron Transfer upon Selective Femtosecond Excitation of Pigments in Membranes of *Heliobacillus mobilis*

Ursula Liebl,[‡,§] Jean-Christophe Lambry,[‡] Winfried Leibl,[§] Jacques Breton,[§] Jean-Louis Martin,[‡] and Marten H. Vos*[,‡]

Laboratoire d'Optique Appliquée, INSERM U451, CNRS URA 1406, Ecole Polytechnique-ENSTA, 91120 Palaiseau, France, and SBE/DBCM, CEN de Saclay, 91191 Gif-sur-Yvette Cedex, France

Received February 26, 1996; Revised Manuscript Received May 6, 1996[⊗]

ABSTRACT: Excitation energy transfer steps in membranes of *Heliobacillus mobilis* were directly monitored by transient absorption spectroscopy with a time resolution of 30 fs under selective excitation within the inhomogeneously broadened bacteriochlorophyll *g* Q_Y band. The initial anisotropy was found to be >0.4, indicating that the pigments are excitonically coupled. After initial decay of this anisotropy in <50 fs, major sub-picosecond components associated with spectral equilibration were identified, corresponding to uphill energy transfer with a 300 fs time constant (812 nm excitation) and downhill energy transfer with 100 and 500 fs components (770 nm excitation). These equilibrations are ascribed predominantly to single excitation transfer steps, as anisotropy measurements showed that equilibration within spectrally similar pigments occurs on the same time scale as spectral equilibration, a situation which contrasts with that in photosystem I. Downhill energy transfer occurs to a significant extent directly to an energetically heterogeneous population of excited states as well as in a sequential way via gradually lower-lying pools of bacteriochlorophyll *g*. This finding supports a description in which all pigments, including the blue-most absorbing, are spatially organized in a random way rather than in clusters of spectrally similar species. Spectral equilibration is not entirely completed prior to formation of the primary radical pair $P798^+A_0^-$, which was found to proceed in a multiexponential way (time constants of 5 and 30 ps). No indication for the formation of radical species other than $P798^+A_0^-$ on the time scale up to 100 ps was found.

The bacteriochlorophyll pigments bound to photosynthetic proteins are involved in both energy transfer and primary photochemistry, processes which have an extremely high overall quantum efficiency. The bulk of these pigments serves to capture photons and to transfer the resulting excited state energy to the pigments constituting the primary donor, where photochemistry starts. As a general feature, the excited state for most pigments has a higher energy than the primary donor and for a minority of pigments it has a lower energy. Such an arrangement is thought to optimize the overall efficiency of photosynthesis (Trissl, 1993).

In the photosynthetic membrane of purple bacteria and in photosystem II (PS II),[1] the two functions of energy and electron transfer, respectively, take place in distinct entities, the light-harvesting and reaction center complexes, and can therefore be studied separately. By contrast, in PS I and in the photosystems of heliobacteria and green sulfur bacteria, a pigment−protein complex exists in which both processes take place. Within this group of photosystems, the heliobacteria are unique in that all energy transfer and primary electron transfer occurs in a single bacteriochlorophyll-containing protein complex, called the reaction center−antenna complex (RC) [for recent reviews, see Amesz (1995), Blankenship (1994), and van Grondelle et al. (1994)]. This complex binds a limited number of pigments (∼50, see below) and can be studied directly in membrane fragments.

The most extensively studied representatives of the heliobacteria, *Heliobacterium chlorum* (Gest & Favinger, 1983) and *Heliobacillus mobilis* (Beer-Romero & Gest, 1987) (the latter is used in the present study), have virtually identical spectroscopic properties (Beer-Romero et al., 1988). The RC core is a homodimer (Liebl et al., 1993), as is that of green sulfur bacteria (Büttner et al., 1992), in contrast to the heterodimeric protein core of PS I and all other RCs known. The heliobacterial RC binds approximately 50 molecules of bacteriochlorophyll (Bchl) *g*, a type of Bchl found only in heliobacteria (Brockmann & Lipinski, 1983). Primary electron transfer occurs from the primary donor P798, a dimer of Bchl *g* [or Bchl *g*′, see van de Meent et al. (1990)], to the primary acceptor A_0, identified as 8^1-hydroxychlorophyll *a* (van de Meent et al., 1991). The overall process of energy transfer to P798 and charge separation has been reported to occur in 20−30 ps (Trost & Blankenship, 1989; van Noort et al., 1992; Lin et al., 1994a). Due to the spectral overlap of P798 with other Bchl *g* pigments, the intrinsic $P798^*A_0 \rightarrow P798^+A_0^-$ charge separation time (P798* denoting the singlet excited state of P798) cannot be measured independently. Using trap-limited energy transfer models, this time has been estimated to be less than 1.2 ps (Lin et al., 1994a), which is somewhat faster than the primary charge separation in wild type RCs of purple bacteria (Martin & Vos, 1992).

The absorption spectrum of the membrane-bound RC complex has a dominant Bchl *g* Q_Y band with a maximum

‡ INSERM U451.

§ SBE/DBCM.

⊗ Abstract published in *Advance ACS Abstracts,* July 1, 1996.

[1] Abbreviations: Bchl, bacteriochlorophyll; DAS, decay-associated spectrum; EDTA, ethylenediaminetetraacetic acid; FMO, Fenna−Matthews−Olson; fwhm, full width at half-maximum; LH1, light-harvesting complex 1; MOPS, 3-(*N*-morpholino)propanesulfonic acid; PMS, *N*-methyldibenzopyrazine methosulfate; PS, photosystem; RC, reaction center; SVD, singular value decomposition.

S0006-2960(96)00462-X CCC: $12.00

at 788 nm and a width of ∼40 nm (∼650 cm^{-1}) (see Figure 2A). The band is inhomogeneously broadened, and analysis of the low-temperature absorption spectrum has led to the assignment of three different pools of pigments (van Dorssen et al., 1985), called Bchl *g* 778, 793, and 808 after their respective absorption maxima. These pools must be considered as the minimal number of spectroscopically distinct pigments, as in principle all pairs of symmetry-related pigments have a different protein environment. Indeed, evidence for spectroscopically distinct pigments within the Bchl *g* 808 pool has been found in low-temperature transient absorption studies (van Noort et al., 1994; Lin et al., 1994b; U. Liebl, J.-C. Lambry, W. Leibl, J. Breton, J.-L. Martin, and M. H. Vos, to be published).

The 650 cm^{-1} width of the 788 nm absorption band is substantially larger than k_BT (240 cm^{-1} at room temperature), in which k_B is the Boltzmann constant and T the absolute temperature. Therefore, at thermal equilibrium, the excitations are not equally distributed over the pigments. Previous optical studies have indicated that excitations are equilibrated to a population dominated by the most red-absorbing pigments prior to electron transfer (van Dorssen et al., 1985; van Noort et al., 1992; Lin et al., 1994a,b). From the study with the highest time resolution hitherto (200 fs), in which nonselective excitation of higher-lying optical transitions was used, it was concluded that spectral equilibration in the Q_Y band takes place within 1−2 ps (Lin et al., 1994a,b). Whereas sub-picosecond spectral equilibration has been observed in antenna systems of other photosynthetic bacteria [see, for instance, Savikhin et al. (1994), Bradforth et al. (1995), and Visser et al. (1995)], in the context of the often-made comparison with PS I (Amesz, 1995; Blankenship, 1994), we note that spectral equilibration in heliobacteria seems to occur considerably faster than in the PS I core where equilibration times of 3−5 ps were reported (Du et al., 1993; Hastings et al., 1995). The latter times are more than 1 order of magnitude slower than equilibration within pools of pigments with isoenergetic excited states (Du et al., 1993).

In heliobacteria, the pathways and the time scale of energy transfer between individual pigments remain essentially unknown. Selective excitation of pigments with a time resolution higher than the expected energy transfer rate, i.e. ∼100 fs, is required to study these issues. Presumably due to the inherent difficulties related to the necessity to work in a low-signal regime and to pump and probe with spectrally (partially) overlapping pulses, spectroscopic studies of this type have only very recently been applied to the study of energy transfer in photosynthetic antenna systems [see, for example, Savikhin and Struve (1994) and Bradforth et al. (1995)]. Most of them use single-wavelength detection of absorption or fluorescence. However, the most complete information can be obtained when full transient spectra are recorded. In our experiments, we used multicolor transient absorption spectroscopy upon selective excitation in the Q_Y band, either of the Bchl *g* 778 pool or of the Bchl *g* 808 pool, with pulse durations down to 30 fs to study primary processes in *H. mobilis*. This approach allows a characterization of the energy transfer taking place on the time scale of tens of femtoseconds and longer. Furthermore, by comparison of the spectral evolution obtained under different excitation conditions, we have been able to establish that full equilibration may take longer than 1−2 ps, even at room temperature. Finally, we have addressed the question of possible additional early electron transfer intermediates, by simultaneous monitoring of the spectral evolution associated with $P798^+$ formation and A_0^- formation. Our study was performed both at room temperature and at cryogenic temperature. In this paper, we present the room-temperature results.

MATERIALS AND METHODS

Membranes of *H. mobilis* were prepared as described by Liebl et al. (1990). All buffers were degassed and stored under argon. A washing step of the membrane fraction in 20 mM MOPS (pH 7.0) containing 1 mM EDTA was added. The pelleted membrane fragments were resuspended in the above buffer to an optical density, at 788 nm, of ∼2.0 for excitation at 812 nm and of ∼1.0 for excitation at 770 nm. Sodium ascorbate (20 mM) and PMS (10 μM) were added to keep P798 reduced during the measurements. Measurements were performed in a cell which was continuously translated perpendicular to the optical beams. The pump and probe beams propagated in a near-parallel configuration through the sample, such that they spatially overlapped essentially over the entire optical path length (1 mm) of the cell.

The general arrangement of the femtosecond spectrometer, operating at 30 Hz, was as described previously (Martin & Vos, 1994; Vos et al., 1996). For the present work, the instrument was set up as follows. To obtain pump pulses centered at 812 and 770 nm, a continuum was amplified using the dyes LDS 821 and LDS 765, respectively, both dissolved in methanol. For pulses at 812 nm, an interference filter was placed in the beam, resulting in a spectrum with a full width at half-maximum (fwhm) of 12 nm. The 770 nm pulses were not filtered and had a fwhm of 25 nm (see Figure 2A). After compression, the pump pulses were near Fourier transform-limited with fwhm times of ∼60 fs (812 nm) and ∼30 fs (770 nm). For most measurements, the probe beam was compressed as described previously (Vos et al., 1996) to an essentially chirp-free (20 fs) continuum over the wavelength range 760−840 nm. For measurements including the 670 nm spectral region, the chirp was minimized at ∼700 nm. Unless stated otherwise, the pump and probe beams had parallel polarization, an arrangement in which the highest signal to noise ratio could be obtained.

We use the relative bleach of the Q_Y band surface after 1 ps (i.e. after most of the initial anisotropy has decayed; see Results) as a measure of the excitation intensity. This method, rather than the number of photons per RC, has been preferred, as the number of Bchl *g* pigments per RC is not unequivocally determined [using different methods, it has been estimated at 35−65 (Vos et al., 1989; Trost & Blankenship, 1989; van de Meent et al., 1990, 1991; Deinum, 1991)]. For most experiments, the intensity of the pump beam was adjusted so that 1 ps less than 0.8% of the Q_Y band surface was bleached, taking a ground state band width of 40 nm. For comparison, assuming (a) a photosynthetic unit size of 35 Bchl *g* per RC, (b) equal oscillator strength of the antenna Bchl *g*'s, and (c) no contribution from stimulated emission to the signal, we find that 0.8% of the Q_Y band surface corresponds to ∼0.3 photon per RC. In this regime, all signals were found to be linear with excitation intensity. Since triplet decay occurs in ∼35 μs (Smit et al.,

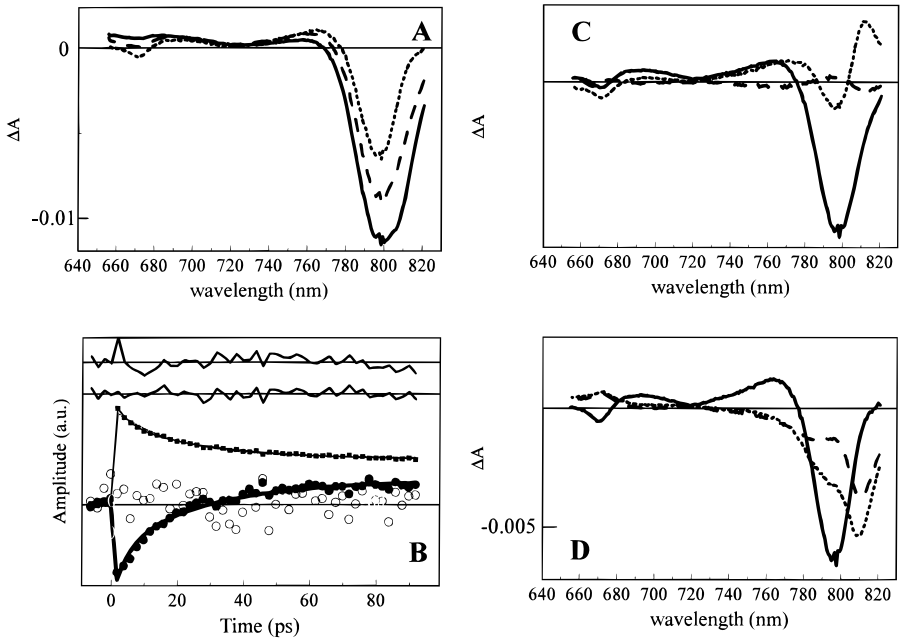

FIGURE 1: Transient absorption spectra and analysis for data obtained in the 655−820 nm range with a time resolution of 2 ps per spectrum upon excitation at 770 nm: (A) transient spectra at selected delay times of 1 ps (—), 11 ps (− −), and 91 ps (- - -), and (B) kinetics of the first (■), second (●), and third (○) SVD component of the entire data set. Solid lines are fits with two experimental (5 and 30 ps). The dashed line is a single exponential (18 ps) fit of the first component. Upper traces are residuals (×5) of the single- (upper) and double-exponential fits of the first component. (C) Spectra of the first (—), second (− −), and third (- - -) SVD component of the entire data set. The kinetics and spectra of the SVD components in panels C and D are both weighted by the square root of the corresponding singular values. (D) Decay-associated spectra of the 5 ps (− −), 30 ps (- - -), and constant (—) components.

1987), singlet−triplet annihilation cannot play a role in our 30 Hz repetition rate experiments.

Data were taken in three different scan types: 1 ps full scale, 100 ps full scale, and 4/50 ps double-time scale. The results were analyzed using singular value decomposition [SVD, see Press et al. (1989)] in a way similar to that described by Nagarajan et al. (1993). Briefly, in SVD, the entire data set $\Delta A(\lambda,t)$ is written, in matrix form, as

$$\Delta A(\lambda,t) = \mathbf{USV}^T \tag{1}$$

If we have m wavelengths and n time points in our data set ($m > n$), **U** is an $m \times n$ matrix containing n basis spectra $A_i(\lambda)$ and **V** an $n \times n$ matrix containing the corresponding n kinetic traces $K_i(t)$. **S** is an $n \times n$ diagonal matrix containing the n singular values s_i, which decay monotonically with i. In other words, the data set can be written as

$$\Delta A(\lambda,t) = \sum_{i=1}^{n} s_i K_i(t) A_i(\lambda) \tag{2}$$

Usually, only the first few components deviate significantly from zero. In this way, the data are reduced to a convenient form, filtering out random noise and correlated noise (noise in the kinetics which has the same profile for all wavelengths). Also, the number of significant SVD components determines the minimum number of independent processes to be considered to describe the entire data set, irrespective of a kinetic model.

Subsequently, the kinetic components $K_i(t)$ were fit with functions of the form $\sum_{j=1}^{p} \alpha_{ij} \exp(-k_j t)$, convoluted with the instrument response function. The minimal number of exponentials p necessary to fit together all SVD components from the scans on all different time scales was determined iteratively. From these fits, decay-associated spectra (DAS) were constructed using eq 2:

$$\mathrm{DAS}_j(\lambda) = \sum_i \alpha_{ij} s_i A_i(\lambda) \tag{3}$$

The different steps of the procedure are illustrated in Figure 1.

We stress that, whereas this method is a convenient data reduction method that allows extraction of the spectral evolution on the different time scales covered by these experiments, it must be kept in mind that the underlying processes do not necessarily proceed exponentially.

RESULTS

Electron Transfer. We first present results obtained on the 100 ps time scale on a spectral range which comprises both the main absorption band at 788 nm and the spectral region around 670 nm where the electron acceptor A_0 absorbs (Nuijs et al., 1985). The spectra were taken with time intervals of 2 ps; therefore, sub-picosecond processes are unresolved. Figure 1A shows transient spectra at various delay times upon excitation at 770 nm. The decay and blue shift of the main bleaching around 800 nm occur concomitantly with the appearance of the bleaching at 670 nm.

The data allow a simultaneous analysis of the entire spectral region as described in Materials and Methods. Panels B and C of Figure 1 show the kinetics and spectra of the first three SVD components. In this case, the third component consists of (wavelength-correlated) noise and only the first two SVD components are significant. This implies that two states are sufficient to describe the spectral evolution on this time scale: the excited state on the time scale of ~2 ps after the pulse and the long time charge-separated state $P798^+A_0^-$. The first component can be fit with a single exponential with a time constant of 18 ps. However, judging

from the residuals (Figure 1B, upper traces), a biexponential decay function, with time constants of 5 and 30 ps, yields a significantly better fit. The second SVD component can also be fit with these time constants. The DAS of the two exponential decay components and the constant component are depicted in Figure 1D. The two decay components are very similar in shape, indicating that formation of the state $P798^+A_0^-$ originates from a similar distribution of excited states on the two time scales. Also, the DAS are very similar in the 670 nm region, and no wavelength dependence of the kinetics was found within the band, such as reported earlier for excitation at 780 nm (Lin et al., 1994a). The ensemble of data can thus be described by the nonexponentially occurring process Bchl $g^* \rightarrow P798^+A_0^-$ without the need to invoke any further state.

Similar experiments were performed for excitation at 812 nm (not shown). Here also, two exponentials with similar spectral properties were needed to fit the data. Time constants of 5 and 30 ps could also be used to describe the data.

Spectral Evolution in the 800 nm Region. To investigate in detail the energy transfer pathways, the spectral evolution in the Bchl *g* Q_Y band region was measured on the sub-picosecond and picosecond time scales using probe pulses compressed at 800 nm. The ground state spectrum and transient spectra at selected delay times for excitation at 770 and 812 nm are shown in Figure 2. The transient spectra at sub-picosecond delay times obtained under the two excitation conditions are very different from each other, indicating that the excitations are not spectrally equilibrated. On this time scale, a blue shift of the initial bleaching occurs upon excitation at the low-energy side of the band and a red shift upon excitation at the high-energy side of the band. This presumably reflects net energy migration, energetically uphill and downhill, respectively, toward an equilibrium distribution. After a few picoseconds, under both excitation conditions, the bleaching extends from ~780 to ~820 nm, indicating that the excitations are distributed over the pigments absorbing at $\lambda >$ ~780 nm, i.e. mostly on Bchl *g* 793 and 808. Even on the time scale of a few picoseconds, some excitation wavelength-dependent spectral evolution takes place; the maximum bleaching blue shifts between 1 and ~4 ps upon excitation at 812 nm, whereas it red shifts upon excitation at 770 nm. After ~4 ps, the transient spectra are very similar but not identical (see Figure 7).

Figure 3 displays the sub-picosecond kinetics at selected wavelengths. They highlight the very fast (<40 fs) initial decay in the spectral region of excitation and the subsequent kinetics on either side of the Q_Y band on the time scale of hundreds of femtoseconds, which are not completed after 1 ps. The kinetics shown in Figure 4, on the longer (4 and 50 ps) time scales, further show that the equilibration takes place up to at least 4 ps (compare kinetics at 784 nm upon excitation at 812 and 770 nm). The kinetics on the time scale of tens of picoseconds, reflecting energy migration to P798 and charge separation, are very similar, but not identical, and can be described with the same time constants.

DAS were obtained from the 4/50 ps data set employing the general procedure described in Materials and Methods and illustrated in Figure 1 for the 100 ps time scale. In this procedure, the 1 and 100 ps scans were also taken into account for a more accurate determination of the shortest and longest time constants. For the full analysis, up to four

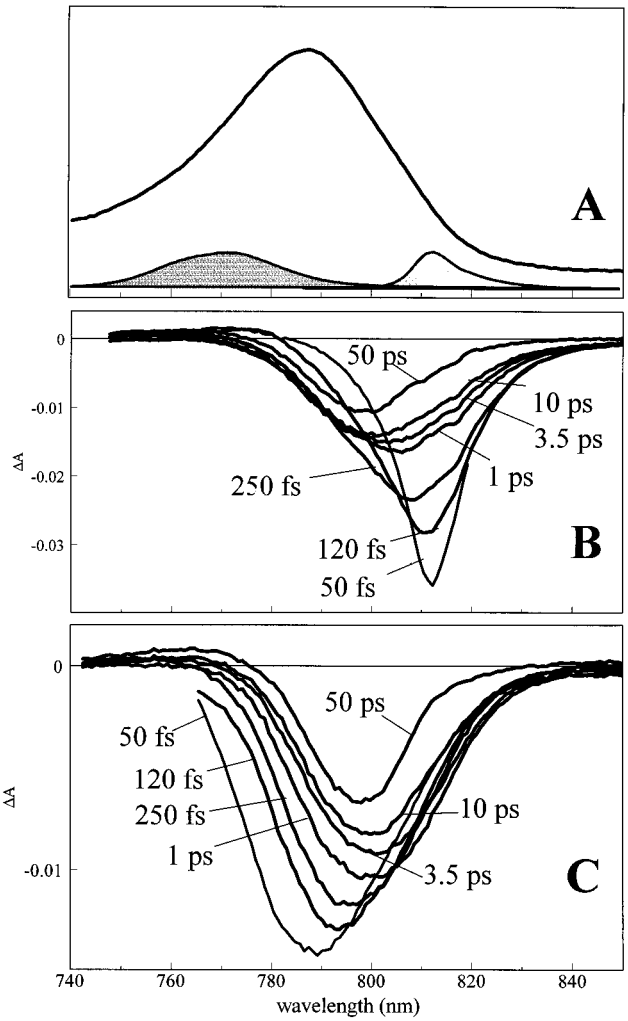

FIGURE 2: Ground state (A) and transient absorption spectra in the Bchl *g* Q_Y band region upon excitation at 812 nm (B) and 770 nm (C). Hatched curves in panel A are spectral profiles of the respective excitation pulses.

SVD components were taken into account. A minimum of five (812 nm excitation) and six (770 nm excitation) exponential decay components was needed to accurately describe the ensemble of data. The fastest component (<40 fs) will be discussed below. The DAS of the other components are depicted in Figure 5. The sub-picosecond components are characterized by asymmetric blue (812 nm excitation) and red shifts (770 nm excitation). Whereas one such component (time constant of 300 fs, isosbestic point at 796 nm) was sufficient to fit the 812 nm excitation data, a minimum of two components (100 and 500 fs with isosbestic points at 796 and 805 nm) was needed to fit the 770 nm excitation data. The two latter shift components do not have the same spectral shape, but they show considerable overlap. It will be discussed that these shapes are consistent with a model of heterogeneous energy transfer.

To investigate whether the observed multiexponential sub-picosecond kinetics for excitation at 770 nm are due to photoselection effects, isotropic data (with the probe beam polarized at magic angle, 54.7°, with respect to the pump beam) were also taken under those excitation conditions. At least two sub-picosecond components were also needed to describe these data, again with best fits with time constants of 100 and 500 fs. This shows that the observed multi-exponentiality is not due to a photoselection effect. The DAS

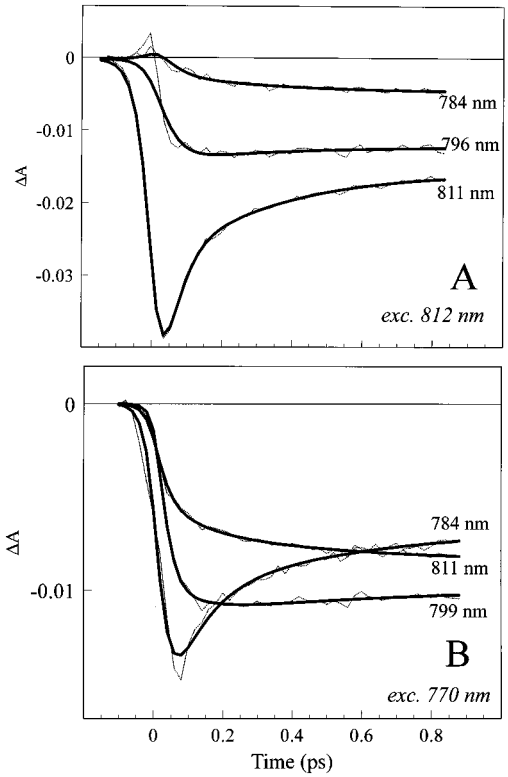

FIGURE 3: Sub-picosecond kinetics (···) at selected wavelengths upon excitation at 812 nm (A) and 770 nm (B). Exponential fits (—) with time constants from the global analysis as described in the text.

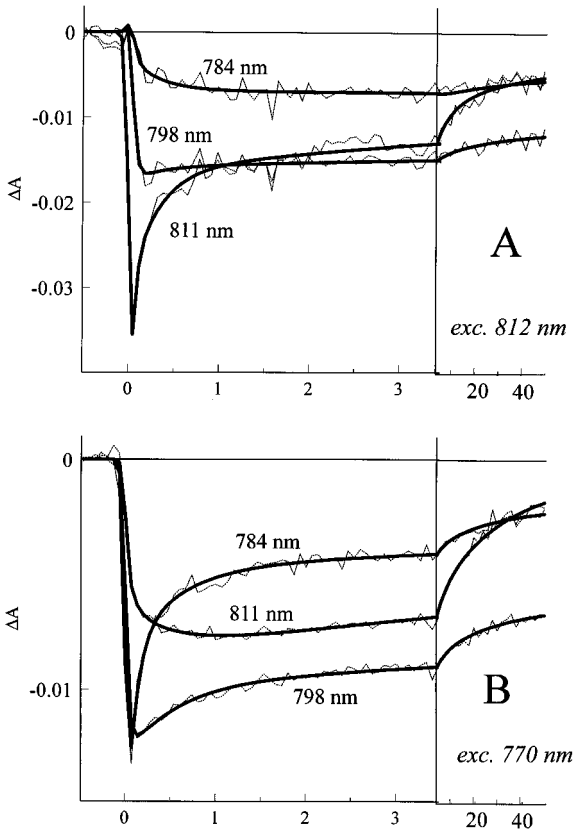

FIGURE 4: Kinetics on the 4 and 50 ps time scales (···) at selected wavelengths upon excitation at 812 nm (A) and 770 nm (B). Exponential fits (—) with time constants from the global analysis as described in the text.

of these components (Figure 5B, inset) are red shifts that are more symmetric than the ones obtained under parallel

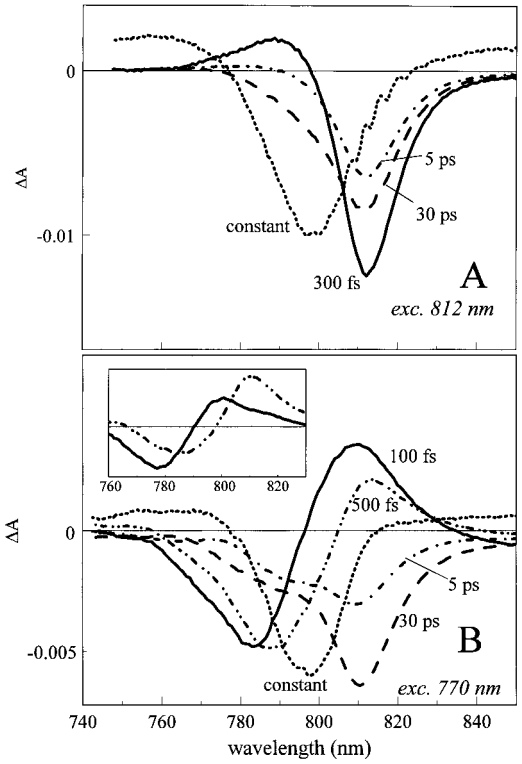

FIGURE 5: Decay-associated spectra (DAS) in the Bchl *g* Q_Y band region upon excitation at 812 nm (A) and 770 nm (B). (Inset) DAS of the sub-picosecond components obtained under magic-angle polarization upon excitation at 770 nm.

polarization conditions. The shape of the slower components is similar to that observed under parallel excitation conditions (not shown).

As mentioned above, the spectral evolution on the picosecond time scale, reflecting the processes of energy transfer to P798 and formation of $P698^+A_0^-$, can be described by two exponential components (time constants of 5 and 30 ps) with similar spectral characteristics, consisting of a net decrease of the (bleaching/stimulated emission) signal. In contrast to the DAS of the 812 nm excitation data, the DAS of the 770 nm excitation data display a shoulder at ~790 nm. Although it cannot be excluded that photoselection effects contribute to this difference, this may indicate that the distributions of excitations from which energy transfer to P798 takes place are more blue-shifted for the case of the 770 nm excitation than for the 810 nm excitation, even on the time scale of 30 ps.

Under both excitation conditions, a very fast component (<40 fs) was needed in the fit (not shown). It decays essentially within the instrumental response function, and a time constant cannot be well-established. Therefore, and because the remaining chirp (~20 fs between 760 and 840 nm) is on the same time scale, the DAS of this component strongly depends on the fit conditions (time interval and imposed time constant). It seems to contain a band shift-like feature, resembling those of the sub-picosecond components discussed above for excitation at either side of the band, and it cannot be excluded that some initial spectral equilibration or nuclear motion takes place on this time scale. Nevertheless, the main feature is always a major strong bleaching at the spectral region of the pump pulse, as can be seen from the kinetics at individual wavelengths (Figure 3). The strong polarization (see below) of this feature may

indicate that it reflects, at least in part, decay of electronic coherence between exciton levels.

Depolarization Dynamics. To investigate the time scale of energy transfer among spectrally similar pigments, the polarization of the transient absorption signals was measured upon excitation at 770 nm. Figure 6A shows the anisotropy in the blue part of the Q_Y band, at 782 nm. The anisotropy $r = (\Delta A_{\|} - \Delta A_{\perp})/(\Delta A_{\|} + 2\Delta A_{\perp})$ and after ~50 fs has a value close to 0.4, the theoretical initial value for uncoupled pigments prior to energy transfer and rotation. This indicates that the excitations have not moved to other pigments to a significant extent on the time scale of <50 fs. The anisotropy decays for a major part on the hundreds of femtoseconds time scale, i.e. roughly with the same kinetics as energy transfer to the more red-absorbing pigments. The data in Figure 6A after ~50 fs can be fit well with a single-exponential decay function, with a time constant of 350 fs and an asymptotic value of 0.05. This decay is within the noise indistinguishable from that of the absorption decay at this wavelength, which was determined with a better signal to noise ratio and described by a biexponential function. We note that the asymmetric shapes of the DAS of the sub-picosecond components obtained with parallel pump and probe beams are also consistent with a loss of anisotropy during the spectral equilibration.

At very early delay times (less than 50 fs), the anisotropy has a value significantly higher than 0.4. The maximum value found in our experiment is 0.52 ± 0.03, and this value may be limited by our time resolution (note that the signal to noise ratio of the raw anisotropy data is significantly higher at early positive times due to the higher amplitude of the signal in $\Delta A_{\|}$ at those times, cf. Figure (3B). Such high values for the initial anisotropy (r_0) were also found at wavelengths not overlapping with the pump spectrum (Figure 6B), indicating that optical coherence between pump and probe pulses in the medium is not (only) at the origin of this high r_0. A possible explanation for the initial anisotropy decay (in less than 30 fs) is that it reflects decay of the electronic coherence between different excitonic levels, coherently excited by the broad-band pump pulse. For comparison, several recent experimental observations of initial anisotropies greater than 0.4 with a subsequent ultrafast decay (Galli et al., 1993; Savikhin & Struve, 1994; Edington et al., 1995) have been interpreted in the theoretical framework of electronic coherence between excitonically coupled transitions (Knox & Gülen, 1993; Wynne & Hochstrasser, 1993; Struve, 1995).

Multiple Excitations. Additional insight into the dynamics of excitation migration within the pigment complex can be gained by studying singlet−singlet annihilation. When more than one excited state is created per RC, and an excitation migrates to a state already occupied, the two excitations will annihilate in one. The rate of annihilation is proportional to the probability of two excitations meeting, which is a function of the number of excitations in the complex, the effective number of accessible states, and the hopping rates. Some experiments were therefore performed with excitation pulses well above the linear regime, where more than one photon is absorbed per RC (not shown). In this case, the initial bleaching/emission signal strongly decays on the time scale of 1−2 ps, indicating that excitation annihilation occurs on this time scale. This is roughly consistent with a single-step energy transfer rate of ~100 fs and an effective domain size at room temperature of ~12 (Lin et al., 1994). However, the overall decay toward the state $P798^+A_0^-$ also speeds up. At an excitation density resulting in the bleaching of ~13% of the Q_Y band, a slowest decay time of ~12 ps was found. The higher net rate of P798* formation on the time scale of ~10 ps implies that not all excitations are annihilated within a few picoseconds. This finding provides a further indication that equilibration toward some excited states is considerably slower than a few hundred femtoseconds.

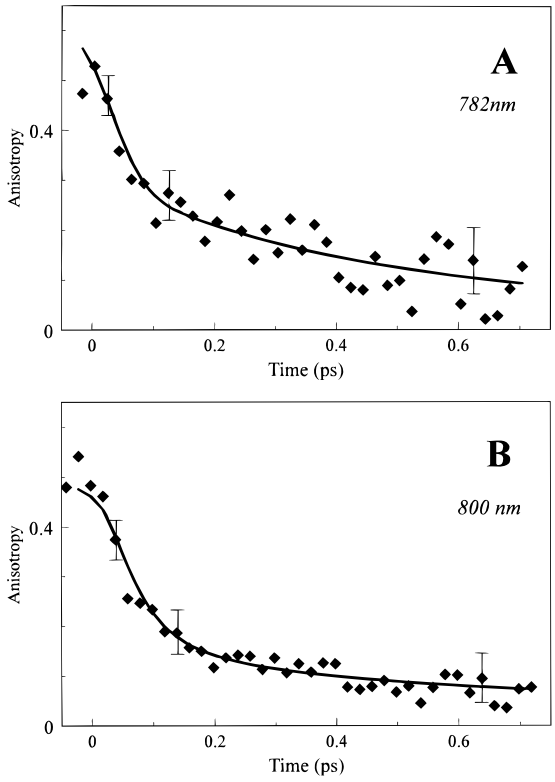

FIGURE 6: Anisotropy of transient absorption at 782 nm (A) and 800 nm (B) upon excitation at 770 nm. The "deconvoluted" anisotropy decay function $r(t)$ cannot be obtained by direct fitting and was obtained as follows. The isotropic data ($\Delta A_{\|} + 2\Delta A_{\perp}$) were fit to a multiexponential decay function $K(t)$ convoluted with the instrument response function $I(t)$. Subsequently, the anisotropic data ($\Delta A_{\|} - \Delta A_{\perp}$) were fit to $r(t)K(t)$, convoluted with $I(t)$, in which the coefficients for $K(t)$ were kept fixed and $r(t)$ was assumed to be a biexponential function. This procedure is similar to that described by Bradforth et al. (1995). Any values less than 30 fs for the shortest time constant for $r(t)$ yielded similar quality fits. An initial anisotropy significantly greater than 0.4 was always found for both wavelengths. The solid lines represent the convoluted anisotropy data, reconstructed from the fits with time constants for $r(t)$ of 20 and 350 fs (A) and 30 and 500 fs (B).

DISCUSSION

The results presented in this paper give insight into the overall processes of energy transfer and primary electron transfer in membranes of *H. mobilis* occurring in the time range of 30 fs to 100 ps. Previous fluorescence (Trost & Blankenship, 1989) and transient absorption studies of the Bchl *g* Q_Y band using sub-picosecond excitation at 590 and 670 nm (Lin et al., 1994a) and using picosecond excitation in the Q_Y band (van Noort et al., 1992) have shown that spectral equilibration mainly occurs on the time scale of 1−2 ps and that the state $P798^+A_{0-}$ is formed in ~20 ps. Whereas our results are in general agreement with these findings, monitoring full transient spectra upon ultrashort excitation at both sides of the Q_Y band allows us to resolve,

both temporally and spectrally, the uphill and downhill energy transfer processes leading to a spectral equilibrium on a time scale of hundreds of femtoseconds. Our data also establish that the charge separation process cannot be adequately described by a single rate constant.

Spectral Evolution in the First 50 fs. The spectral evolution during the pump−probe overlap is characterized by a large decay of the induced bleaching in the excitation region at both excitation conditions. As mentioned in the Results, the concomitant strong decay in anisotropy (initially >0.4) may reflect decay of electronic coherence between coherently excited exciton states. Nevertheless, it cannot be excluded that some very fast energy transfer or nuclear motions contribute to the dynamics at this time scale. In particular, whereas the 50 fs transient spectrum upon excitation at 812 nm consists of a bleaching signal centered at 812 nm, upon excitation at 770 nm, it is significantly red-shift (to ∼790 nm) with respect to the spectrum of the pump pulse. This shift is more than the bias that would be expected in view of the higher absorption of the RC at the red side of the pump pulse. This may seem to indicate that in the latter case downhill energy transfer occurs on the time scale of <50 fs. However, the anisotropy is still close to 0.4 at 50 fs, indicating that energy transfer has not occurred to a significant extent. Two other explanations can be offered for the initial red-shifted bleaching. First, the signal is expected to bear contributions from both ground state bleaching and from stimulated emission, which is also spectroscopically apparent as a bleaching. If the system propagates out of the initially populated Franck−Condon region in less than 50 fs, the combined signal of bleaching and (red-shifted) stimulated emission is expected to have a maximum more to the red than the ground state bleaching alone. Second, as has been suggested by Smit et al. (1989), the blue tail of the absorption band may be partly due to higher vibrational levels of electronic transitions with a more red-lying maximum. In this case excitation of the higher vibrational levels would indeed result in a red-shifted initial bleaching.

Sub-Picosecond Spectral Equilibration. Our data show that major spectral equilibration processes at room temperature occur on the time scale of hundreds of femtoseconds. This is in general agreement with the estimates for the time scale of energy transfer within other light-harvesting complexes (van Grondelle et al., 1994). The observable downhill and uphill energy transfer occurs roughly on the same time scale, as can be expected for an equilibration process (equilibration between two energetically different species occurs, for both down- and uphill equilibration, with a rate equal to the sum of the two individual rate constants). Excitation at 812 nm creates a distribution of excitations which is relatively close to the thermally equilibrated distribution, reached by uphill energy transfer which can be described with a single rate constant of 300 fs. Excitation at 770 nm creates an excitation population more distinct from the equilibrium population. It results in more complex spectral dynamics reflecting downhill energy transfer, which can be fit with two exponential components of 100 and 500 fs.

An open question is whether the pigments are organized such that energy transfer occurs in a sequential way, first among isoenergetic states and then on longer time scales to spectrally shifted pigments, or, alternatively, whether energy transfer occurs in a random way. Our experiments, and in particular those with excitation at 770 nm, can be interpreted in light of this question.

First, we note that the decay of the anisotropy occurs on the same time scale of a few hundred femtoseconds as the spectral red shift (Figure 6). This feature demonstrates that equilibration between spectrally similar pigments does not take place prior to energy transfer to more red-lying pigments. Therefore, energy transfer from the initially populated excited states appear to occur on the same time scale to both isoenergetic and lower-lying states.

A further question is whether excitations can be transferred directly to all (energetically accessible) different types of pigments. More precisely, for excitation at the blue side of the spectrum, can excitations be transferred directly to the red-most absorbing species, or does transfer occur necessarily via intermediately located species? The analysis in terms of two shift components with a different isosbestic point is consistent with a sequential mechanism, of the type A → B (100 fs) → C (500 fs) (in which A, B, and C might be thought of as Bchl *g* 778, 793, and 808, respectively). However, the DAS of the two components show considerable overlap, and in particular, the kinetics at wavelengths as high as 815 nm have a 100 fs component. It thus seems plausible that the fastest component also reflects some energy transfer to the red-most absorbing pigments. A similar conclusion can be drawn from measurements at 20 K, where the spectral species are more well-separated (unpublished results). The fact that the two components concern roughly the same spectral range, albeit with shifted isosbestic points, indicates that they possibly also reflect heterogeneous energy transfer kinetics. As illustrated by the work on LH1 from purple bacteria (Bradforth et al., 1995; Visser et al., 1995; Somsen et al., 1994), kinetic heterogeneity can be expected when a distribution of excited states is initially populated in a spectrally heterogeneous multichromophore system. In this picture, the observed fastest energy transfer times (∼100 fs) can be identified with single-step excitation transfer times. The slower times (∼500 fs) may reflect a combination of slower direct excitation transfer and multiple-step excitation transfer to the further red-lying pigments. Within this framework, we note that the DAS of the two magic angle components in the 770 nm region (Figure 5B inset) indicate that the excited blue-most absorbing pigments must transfer their energy in ∼100 fs. Altogether, we favor the hypothesis that a significant part of the excitations can be transferred directly to a spectrally random population of pigments, but a scheme of predominantly sequential energy transfer cannot be excluded.

As energy transfer presumably occurs predominantly between excited states located on close-lying pigments, the above reasoning that energy transfer from the highest excited state levels occurs directly to an energetically heterogeneous distribution of states is consistent with a situation in which the organization of the pigments is spatially random with regard to their spectral properties. If only a sequential model in terms of three pigment pools Bchl *g* 778, 793, and 808 is valid (see above), this applies to the organization of Bchl *g* 778 and 793. If some energy transfer occurs directly from Bchl *g* 778 to Bchl *g* 808, as seems to be likely, then at least some of the red-most absorbing pigments are located near the blue-most absorbing ones. A model of spatially nonclustered pigments is in general agreement with the

conclusion of Lin et al. (1994b), derived from low-temperature data, of random rather than funnel-like organization of pigments. While their simulations were only sensitive to the distribution of the red-most pigments (absorbing at greater than ~800 nm), our results also show that indeed the more blue-absorbing pigments are distributed such that they are located in contact with the other pigments, including probably at least some of the red-most absorbing pigments. It thus seems unlikely that they are all concentrated in a cluster.

Nuclear Motions? In the previous discussion, we have assumed that spectral shifts on the time scale of hundreds of femtoseconds reflect interpigment spectral equilibration. We note that spectral changes can also reflect processes within an electronic state. In particular, in the P* state of RCs of purple bacteria, we have shown that the stimulated emission displays an initial red shift in ~150 fs (Vos et al., 1994), reflecting nuclear motion along coordinates coupled to the optical transition. Whereas it cannot be excluded that such effects also contribute to the spectral evolution reported here, two observations indicate that they do not predominantly underlie the shift components. (1) The sign of the shift is opposite for excitation at either side of the absorption band, as expected for spectral equilibration, but not for an emission shift. (2) The extent of the red shift (~30 nm) upon excitation at 770 nm is much larger than that expected for the Stokes shift [estimated at ~10 nm from the low-temperature fluorescence spectrum reported by van Dorssen et al. (1985)].

More generally, the appearance of oscillatory features in the transient kinetics reflecting vibrational motions can be expected, such as was observed in experiments in bacterial RCs (Vos et al., 1991, 1993, 1994; Stanley & Boxer, 1995) and in some antenna systems (Chachisvilis et al., 1994; Savikhin et al., 1994; Bradforth et al., 1995). Such oscillations are not resolved in the present work on *H. mobilis*. Several explanations for this absence of oscillations can be invoked; the most likely is as follows. For motions within a single electronic state, the phase and amplitude of the oscillations are expected to be highly wavelength-dependent (Vos et al., 1993). In the case of the present experiments on *H. mobilis*, the initially populated selection of excited states evolves to a spectrally much more heterogeneous population of excited states on the 100−500 fs time scale; i.e. on the time scale of the periods of the expected (and temporally resolvable) oscillations. Thus, if vibrational coherence is maintained upon energy transfer [which seems possible, cf. Bradforth et al., (1995)], the spectroscopic features would be rapidly canceled out by the superposition of a heterogeneous distribution of phases and amplitudes at each wavelength. For comparison, we note that for chlorosomes of *Chloroflexus aurantiacus*, where kinetic oscillations have been resolved, spectral equilibration does not appear in the sub-picosecond time scale (Savikhin et al., 1994). Also in LH1, where the Q_Y absorption band furthermore is less broadened than in *H. mobilis*, the main isotropic decay was considerably slower (0.5−1 ps) (Bradforth et al., 1995) than in the present study.

Transient Spectra after a Few Picoseconds. At room temperature and in thermal equilibrium, the excitations are expected to be distributed between the Bchl *g* 808 and 793 pigments mainly (Lin et al., 1994a). Thus, excitation at 812 and 770 nm corresponds to populating distributions of excited states that are "cold" and "hot", respectively, with respect to room temperature. After a few picoseconds, the transient spectra have evolved to a similar (but not identical; see below) shape (Figure 7). This shows directly that substantial thermalization of the distribution of the occupied excited states takes place within a few picoseconds. Direct comparison of the transient spectra with those expected for Bchl *g** in thermal (Boltzmann) equilibrium is difficult because of (a) the expected contribution of stimulated emission to the signal, (b) the discrete nature of the involved excited state levels, and (c) possible excitonic coupling between pigments.

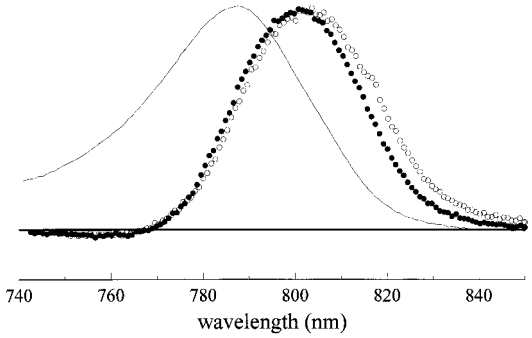

FIGURE 7: Ground state absorption (—) and inverted transient absorption spectra at $t = 3.5$ ps upon excitation at 770 nm (●) and 812 nm (○) redrawn from Figure 2 and normalized.

Whereas substantial spectral equilibration takes place on a time scale of 1−2 ps, after a few picoseconds, the transient spectra obtained upon excitation at the blue side of the Q_Y band are still somewhat blue-shifted compared to those obtained upon red excitation. The spectra at $t = 3.5$ ps reflect a combination of Bchl *g** and $P798^+A_0^-$ (being formed for ~35% at this time delay). Two explanations can be offered for the difference between the spectra: (1) incomplete spectral equilibration and (2) a higher initial overall rate of charge separation upon excitation at the blue side of the spectrum [cf. discussions based on simulations of energy transfer in PS I by Laible et al. (1994), Trinkunas and Holzwarth (1994), and Valkunas et al. (1995)]. In both cases, it is concluded that spectral equilibration is *not* completed prior to charge separation. Thus, some spectral equilibration within the most red-absorbing pigments may take place on a time scale longer than a few picoseconds. Such a slow equilibration has not been identified at room temperature to date. Any equilibration on the picosecond time scale occurs concomitantly with charge separation (for which we found time constants of 5 and 30 ps) and will therefore not appear as a separate phase in our analysis. The somewhat different spectral shapes of the DAS associated with $P798^+A_0^-$ formation on the picosecond time scale upon excitation at 812 and 770 nm (Figure 5) may be due to the small difference in Bchl *g** spectral distribution on the picosecond time scale. It should be noted that the compared transient spectra are obtained with parallel polarization for pump and probe pulses. Whereas we observed very fast depolarization (Figure 6), a possible different residual polarization on the picosecond time scale for the two excitation conditions may bias the comparison.

Kinetics of $P798^+A_0^-$ Formation. The kinetics of formation of $P798^+A_0^-$ from excited Bchl *g* on the picosecond time scale are clearly better described with a non-single-exponential function than with a single-exponential function (Figure 1). For both excitation conditions, the DAS corre-

sponding to the two exponential components (5 and 30 ps) are very similar (Figure 5). In other words, the spectral characteristics do not evolve strongly during the charge separation process. This shows that the nonexponentiality is not due to different transfer times from *spectrally* distinct pools.

An interesting possible origin for the observed nonexponential kinetics of charge separation is that the kinetics of P798* formation are nonexponential. In principle, this can only lead to nonexponential overall kinetics in the diffusion-limited regime of trapping, where the escape rate from P798* to the antenna is much lower than the rate of charge separation. Singlet−singlet annihilation under multiple-excitation conditions prior to charge separation, as we have observed, is consistent with the trap-limited regime of charge separation, as it is also assumed by Lin et al. (1994a). However, it is possible that the individual equilibration rates are strongly heterogeneous, even within spectrally similar pigments. If some excited states are more weakly coupled to the other excited states, equilibration of these states may occur in picoseconds rather than in hundreds of femtoseconds. In this case, they would act as "temporary traps" and slow down part of the overall trapping process. The indications from this work for incomplete equilibration after a few picoseconds support such a mechanism. Also, the observed acceleration of the charge separation under multiple excitation conditions is consistent with such a mechanism.

Other origins for nonexponential kinetics are also possible. For example, the kinetics of the reaction $P798^*A_0 \rightarrow P798^+A_0^-$ may be intrinsically heterogeneous, as it is the case for the kinetics of primary charge separation in reaction centers of *C. aurantiacus* (Martin et al., 1990; Becker et al., 1991) and of purple bacteria (Vos et al., 1991; Du et al., 1992), where the primary donor can be directly excited. Finally, vibrational cooling may occur on the same time scale as charge separation, and consequently, the hopping rates gradually slow down. Decay of vibrational coherence signals observed in membrane-bound RCs of purple bacteria (Vos et al., 1991, 1993, 1994) and in antenna systems (Chachisvilis et al., 1994; Savikhin et al., 1994; Bradforth et al., 1995) has shown that vibrational relaxation may occur on a time scale of at least 2 ps. Summarizing the nonexponential kinetics of charge separation may originate from heterogeneity in the equilibration kinetics, but other origins cannot be ruled out.

Other Redox Intermediates? From our data on the picosecond time scale in the 670 nm region (Figure 1), it appears that the growth kinetics of the bleaching at 670 nm are the same as the decay kinetics in the 800 nm region, indicating that A_0^- is formed with the same kinetics as $P798^+$. A_0^- reoxidation is known to occur with a time constant of ∼600 ps (Nuys et al., 1985; Lin et al., 1994a, 1995; Leibl et al., 1995), which is beyond the time window of this study, and no further electron transfer reactions occurring on the time scale of tens of picoseconds need to be invoked to model our data. This conclusion contrasts with that of Lin et al. (1994a), who measured faster kinetics at 670 nm (upon excitation at 780 nm) than at the Bchl *g* Q_Y band (upon excitation in higher-lying bands) and on the basis of these observations proposed a model in which A_0^- equilibrates in ∼10 ps with another reduced species. The discrepancy may arise from the fact that different excitation conditions and scan times were used in the latter study, whereas our data were taken in one set. Furthermore, judging from the extent of the 670 nm bleaching, the 780 nm excitation experiments by Lin et al. were performed in a regime of rather high excitation densities, where the rate of charge separation may be increased.

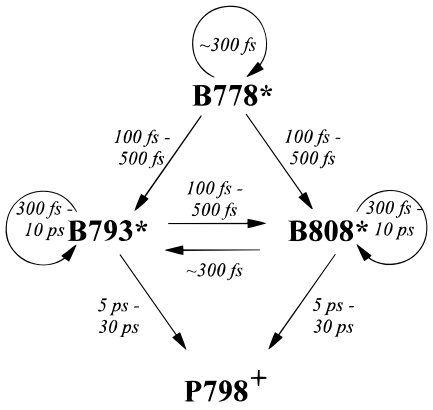

FIGURE 8: Scheme of energy transfer between different bacteriochlorophyll spectral pools and trapping by P798, summarizing the results of this paper. B778, B793, and B808 denote the Bchl *g* 778, 793, and 808 pools, respectively. The circular arrows refer to equilibration within the different pools. The time constants refer to the experimentally observed equilibration and trapping times, not to intrinsic rate constants. The 10 ps time constant for equilibration within the Bchl *g* 793 and 808 pools was not measured directly experimentally but refers to the possible picosecond equilibration as discussed in the text.

Concluding Remarks. Figure 8 summarizes the results of the present study in terms of energy transfer between spectrally different Bchl pools and trapping by P798. We have shown directly that spectral equilibration in *H. mobilis* occurs mainly on the time scale of hundreds of femtoseconds, and probably also to a minor extent on the picosecond time scale. A picture emerges in which energy transfer is a heterogeneous process, i.e. from a given excited state, energy transfer takes place on the same time scale to states with a different energy as to isoenergetic states. This probably reflects a spatially heterogeneous organization of the different spectral types of pigments in the RC.

The heliobacterial photosystem has often been compared to PS I (Amesz, 1995; Blankenship, 1994), and it has been suggested to be its evolutionary ancestor (Liebl et al., 1992). There is a relatively extended literature on energy transfer in a wide variety of different PS I preparations (van Grondelle et al., 1994), but only very recently was a transient absorption study with sub-picosecond selective excitation reported (Hastings et al., 1995). From this study on PS I core preparations, it was inferred that spectral equilibration takes place in 3−5 ps, which is 1 order of magnitude slower than that of the main components in heliobacteria. On the other hand, in an ultrafast fluorescence anisotropy study of PS I, single-step equilibration within spectrally similar pigments has been reported to occur in ∼180 fs (Du et al., 1993), which is similar to the value reported here for *H. mobilis*. From these comparisons, it would thus seem that PS I displays a larger extent of spatial organization of the various spectral species and possibly also a weaker interaction between spectrally different species.

A more general observation is that in PS I many processes, including overall spectral equilibration, $P700^+A_0^-$ formation, and A_0^- reoxidation [which takes only about 30 ps; see Shuvalov et al. (1986), Hecks et al. (1994), and Hastings et

al. (1995)], seem to take place in the time range of ~3 to ~50 ps, whereas in *H. mobilis* membranes, the corresponding processes are well-separated in time and occur over a time span covering more than 3 orders of magnitude (~300 fs to ~600 ps). Thus, the overall kinetic picture of stabilization of the captured photon energy for energy transfer and primary electron transfer in both photosystems is quite different.

REFERENCES

Amesz, J. (1995) in *Anoxygenic Photosynthetic Bacteria* (Blankenship, R. E., Madigan, M. T., & Bauer, C. E., Eds.) pp 687−697, Kluwer, Dordrecht.

Becker, M., Middendorf, V., Nagarajan, V., Parson, W. W., Martin, J. E., & Blankenship, R. E. (1991) *Biochim. Biophys. Acta 1057*, 299−312.

Beer-Romero, P., & Gest, H. (1987) *FEMS Microbiol. Lett. 41*, 109−114.

Beer-Romero, P., Favinger, J. L., & Gest, H. (1988) *FEMS Microbiol. Lett. 49*, 441−454.

Blankenship, R. E. (1994) *Antonie van Leeuwenhoek 65*, 311−329.

Bradforth, S. E., Jimenez, R., van Mourik, F., van Grondelle, R., & Fleming, G. R. (1995) *J. Phys. Chem. 99*, 16179−16191.

Brockmann, H., & Lipinski, A. (1983) *Arch. Microbiol. 136*, 17−19.

Büttner, M., Xie, D.-L., Nelson, H., Pinther, W., Hauska, G., & Nelson, N. (1992) *Proc. Natl. Acad. Sci. U.S.A. 89*, 8135−8139.

Chachisvilis, M., Pullerits, T., Jones, M. R., Hunter, C. N., & Sundström, V. (1994) *Chem. Phys. Lett. 224*, 345−354.

Deinum, G. (1991) Ph.D. Thesis, University of Leiden, The Netherlands.

Du, M., Rosenthal, S. J., Xie, X., DiMagno, T. J., Schmidt, M., Hanson, D. K., Schiffer, M., Norris, J. R., & Fleming, G. R. (1992) *Proc. Natl. Acad. Sci. U.S.A. 89*, 8517−8521.

Du, M., Xie, X., Jia, Y., Mets, L., & Fleming, G. R. (1993) *Chem. Phys. Lett. 201*, 535−542.

Edington, M. D., Riter, R. E., & Beck, W. F. (1995) *J. Phys. Chem. 99*, 15699−15704.

Galli, C., Wynne, K., LeCours, S. M., Therien, M. J., & Hochstrasser, R. M. (1993) *Chem. Phys. Lett. 206*, 493−499.

Gest, H., & Favinger, J. L. (1983) *Arch. Microbiol. 136*, 11−16.

Hastings, G., Reed, L. J., Lin, S., & Blankenship, R. E. (1995) *Biophys. J. 69*, 2044−2055.

Hecks, B., Wulf, K., Breton, J., Leibl, W., & Trissl, H.-W. (1994) *Biochemistry 33*, 8619−8624.

Knox, R. S., & Gülen, D. (1993) *Photochem. Photobiol. 57*, 40−43.

Laible, P. D., Zipfel, W., & Owens, T. G. (1994) *Biophys. J. 66*, 844−860.

Leibl, W., Toupance, B., & Breton, J. (1995) in *Photosynthesis: from Light to Biosphere, Vol. II* (Mathis, P., Ed.) pp 191−194, Kluwer, Dordrecht.

Leibl, U., Rutherford, A. W., & Nitschke, W. (1990) *FEBS Lett. 261*, 427−430.

Liebl, U., Mockensturm-Wilson, M., Trost, J. T., Brune, D. C., Blankenship, R. E., & Vermaas, W. F. J. (1992) in *Research in Photosynthesis, Vol. II* (Murata, N., Ed.) pp 595−598, Kluwer, Dordrecht.

Liebl, U., Mockensturm-Wilson, M., Trost, J. T., Brune, D. C., Blankenship, R. E., & Vermaas, W. F. J. (1993) *Proc. Natl. Acad. Sci. U.S.A. 90*, 7124−7128.

Lin, S., Chiou, H.-C., Kleinherenbrink, F. A. M., & Blankenship, R. E. (1994a) *Biophys. J. 66*, 437−445.

Lin, S., Kleinherenbrink, F. A. M., Chiou, H.-C., & Blankenship, R. E. (1994b) *Biophys. J. 67*, 2479−2489.

Lin, S., Chiou, H.-C., & Blankenship, R. E. (1995) *Biochemistry 34*, 12761−12767.

Martin, J.-L., & Vos, M. H. (1992) *Annu. Rev. Biophys. Biomol. Struct. 21*, 199−222.

Martin, J.-L., & Vos, M. H. (1994) *Methods Enzymol. 232*, 416−430.

Martin, J.-L., Lambry, J.-C., Ashokkumar, M., Michel-Beyerle, M. E., Feick, R., & Breton, J. (1990) in *Ultrafast Phenomena VII* (Harris, C. B., Ippen, E. P., Mourou, G. A., & Zewail, A. H., Eds.) pp 524−528, Springer, Berlin.

Nagarajan, V., Parson, W. W., Davis, D., & Schenck, C. C. (1993) *Biochemistry 32*, 12324−12336.

Nuijs, A. M., van Dorssen, R. J., Duysens, L. N. M., & Amesz, J. (1985) *Proc. Natl. Acad. Sci. U.S.A. 82*, 6965−6968.

Press, W. H., Flannery, B. P., Teukolsky, S. A., & Vetterling, W. T. (1989) *Numerical Recipes*, Cambridge University Press, New York.

Savikhin, S., & Struve, W. S. (1994) *Biochemistry 33*, 11200−11208.

Savikhin, S., Zhu, Y., Lin, S., Blankenship, R. E., & Struve, W. S. (1994) *J. Phys. Chem. 98*, 10322−10334.

Shuvalov, V. A., Nuijs, A. M., van Gorkom, H. J., Smit, H. W. J., & Duysens, L. N. M. (1986) *Biochim. Biophys. Acta 850*, 319−323.

Smit, H. W. J., Amesz, J., & van der Hoeven, M. F. R. (1987) *Biochim. Biophys. Acta 893*, 232−240.

Smit, H. W. J., van Dorssen, R. J., & Amesz, J. (1989) *Biochim. Biophys. Acta 973*, 212−219.

Somsen, O. J. G., van Mourik, F., van Grondelle, R., & Valkunas, L. (1994) *Biophys. J. 66*, 1580−1596.

Stanley, R. J., & Boxer, S. G. (1995) *J. Phys. Chem. 99*, 859−863.

Struve, W. S. (1995) in *Anoxygenic Photosynthetic Bacteria* (Blankenship, R. E., Madigan, M. T., & Bauer, C. E., Eds.) pp 297−313, Kluwer, Dordrecht.

Trissl, H.-W. (1993) *Photosynth. Res. 35*, 247−263.

Trost, J. T., & Blankenship, R. E. (1989) *Biochemistry 28*, 9898−9904.

Valkunas, L., Liuolia, V., Dekker, J. P., & van Grondelle, R. (1995) *Photosynth. Res. 43*, 149−154.

van de Meent, E. J., Kleinherenbrink, F. A. M., & Amesz, J. (1990) *Biochim. Biophys. Acta 1015*, 223−230.

van de Meent, E. J., Kobayashi, M., Erkelens, C., van Veelen, P. A., & Amesz, J. (1991) *Biochim. Biophys. Acta 1058*, 356−362.

van Dorssen, R. J., Vasmel, H., & Amesz, J. (1985) *Biochim. Biophys. Acta 809*, 199−203.

van Grondelle, R., Dekker, J. P., Gillbro, T., & Sundström, V. (1994) *Biochim. Biophys. Acta 1187*, 1−65.

van Noort, P. I., Aarstma, T. J., & Amesz, J. (1992) *Biochim. Biophys. Acta 1140*, 15−21.

van Noort, P. I., Aarstma, T. J., & Amesz, J. (1994) *Biochim. Biophys. Acta 1184*, 21−27.

Visser, H. M., Somsen, O. J. G., van Mourik, F., Lin, S., van Stokkum, I. H. M., & van Grondelle, R. (1995) *Biophys. J. 69*, 1083−1099.

Vos, M. H., Klaassen, H. E., & van Gorkom, H. J. (1989) *Biochim. Biophys. Acta 973*, 163−169.

Vos, M. H., Lambry, J.-C., Robles, S. J., Youvan, D. G., Breton, J., & Martin, J.-L. (1991) *Proc. Natl. Acad. Sci. U.S.A. 88*, 613−617.

Vos, M. H., Rappaport, F., Lambry, J.-C., Breton, J., & Martin, J.-L. (1993) *Nature 363*, 320−325.

Vos, M. H., Jones, M. R., Hunter, C. N., Breton, J., & Martin, J.-L. (1994) *Proc. Natl. Acad. Sci. U.S.A. 91*, 12701−12705.

Vos, M. H., Jones, M. R., Breton, J., Lambry, J.-C., & Martin, J.-L. (1996) *Biochemistry 35*, 2687−2692.

Wynne, K., & Hochstrasser, R. M. (1993) *Chem. Phys. 171*, 179−188; *Ibid. 173*, 539 (erratum).

BI960462I